BIOCHEMISTRY
including biophysical chemistry & molecular biology

Article

pubs.acs.org/biochemistry

Activity-Based Protein Profiling of the *Escherichia coli* GlpG Rhomboid Protein Delineates the Catalytic Core

Allison R. Sherratt,[†] David R. Blais,[‡] Houman Ghasriani,[§] John Paul Pezacki,*[,†,‡,§] and Natalie K. Goto*[,†,§]

[†]Department of Biochemistry, Microbiology and Immunology, University of Ottawa, Health Sciences Campus, 451 Smyth Road, Ottawa, Canada K1H 8M5

[‡]Steacie Institute for Molecular Sciences, National Research Council of Canada, 100 Sussex Drive, Ottawa, Canada K1A 0R6

[§]Department of Chemistry, University of Ottawa, 10 Marie-Curie, Ottawa, Canada K1N 6N5

Supporting Information

ABSTRACT: Rhomboid proteins comprise the largest class of intramembrane protease known, being conserved from bacteria to humans. The functional status of these proteases is typically assessed through direct or indirect detection of peptide cleavage products. Although these assays can report on the ability of a rhomboid to catalyze peptide bond cleavage, differences in measured hydrolysis rates can reflect changes in the structure and activity of catalytic residues, as well as the ability of the substrate to access the active site. Here we show that a highly reactive and sterically unencumbered fluorophosphonate activity-based protein profiling probe can be used to report on the catalytic integrity of active site residues in the *Escherichia coli* GlpG protein. We used results obtained with this probe on GlpG in proteomic samples, in combination with a conventional assay of proteolytic function on purified samples, to identify residues that are located on the cytoplasmic side of the lipid bilayer that are required for maximal proteolytic activity. Regions tested include the 90-residue aqueous-exposed N-terminus that encompasses a globular structure that we have determined by solution nuclear magnetic resonance, along with residues on the cytoplasmic side of the transmembrane domain core. While in most cases mutation or elimination of these residues did not significantly alter the catalytic status of the GlpG active site, the lipid-facing residue Arg227 was found to be important for maintaining a catalytically competent active site. In addition, we found a functionally critical region outside the transmembrane domain (TMD) core that is required for maximal protease activity. This region encompasses an additional 8−10 residues on the N-terminal side of the TMD core that precedes the first transmembrane segment and was not previously known to play a role in rhomboid function. These findings highlight the utility of the activity-based protein profiling approach for the characterization of rhomboid function.

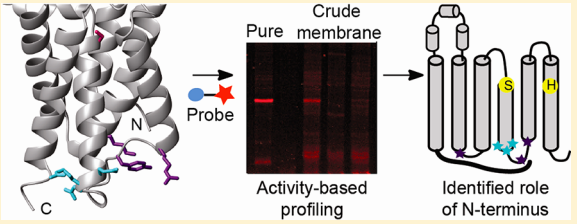

Rhomboids are unique integral membrane proteins that use a serine protease mechanism to cleave transmembrane substrates within the lipid bilayer. This large intramembrane protease group is nearly ubiquitous across all kingdoms,[1,2] and although only a fraction has been assigned a function, the prospective medical importance of the rhomboid family has become widely appreciated.[3,4] This is supported by the rhomboid's role in cell signaling,[5,6] mitochondrial remodeling,[7,8] apoptosis,[9,10] activation of signal translocation in bacteria,[11] host cell invasion by apicomplexan parasites that cause malaria and toxoplasmosis,[12] and immune system evasion in parasitic amoeba.[4,13] In addition to identification of these diverse functions, an abundance of structural and functional data has been obtained, allowing the development of a cohesive model that explains how a TM helix substrate in the normally water-poor environment of the lipid membrane can be cleaved (reviewed in refs 14 and 15).

One aspect of rhomboid function that is still not well understood is the potential role of extramembraneous domains in modulating rhomboid function. Many rhomboids contain N- and/or C-terminal soluble domains that vary in size, sequence, and putative function.[2] In some cases, these domains appear to influence substrate specificity or protease activity, with the most well-characterized example being human RHBDL2. This rhomboid cleaves thrombomodulin, but only when both its cytoplasmic domain and that of the thrombomodulin are present.[16] The *Escherichia coli* and *Pseudomonas aeruginosa* GlpG rhomboids also have cytoplasmic domains that appear to be important for maximal activity, with the removal of this domain reducing the rate of protein hydrolysis.[17,18] However, structures of a full-length GlpG rhomboid from either system are not available, with removal of the cytoplasmic domain being required for crystallization.[18−24] Consequently, it is not yet known how sequences outside the rhomboid core domain can influence the activity of the catalytic site.

Received: March 19, 2012
Published: September 10, 2012

   dx.doi.org/10.1021/bi301087c | *Biochemistry* 2012, 51, 7794−7803

One way to directly probe the activity of enzyme catalytic sites that we have used in this work is based on the activity-based protein profiling (ABPP) approach typically used for high-throughput analyses of enzyme families in complex proteomic samples. ABPP usually involves activity-based probes (ABPs) that target and chemically modify the active site of groups of enzymes (reviewed in refs 24−28). This approach has been applied successfully to important problems related to human health, such as cancer, neurobiology, parasitology, and virology.[24−28] A variety of enzyme classes have also been studied using this technique, including proteases, kinases, phosphatases, lipid transferases, and histone deacetylase enzymes.[26−29] For the study of serine hydrolases, fluorophosphonate (FP)-containing activity-based probes have demonstrated great utility, having been used extensively in cell culture and diverse tissue types,[30−34] to identify inhibitors of enzyme function,[30,35] and to functionally annotate enzymes of unknown function.[36,37] One advantage of this class of mechanism-based suicide inhibitors is their small size, because their reaction with the nucleophilic serine hydroxyl group is not restricted by substrate specificities of target enzymes. Moreover, when the FP probe is linked to a fluorescent marker such as rhodamine, polyacrylamide gel analysis of ABP-treated proteomic samples allows the activity of specific enzyme targets to be characterized without the need for purification. Herein we have used a rhodamine-tagged FP probe in ABPP experiments, in combination with other approaches, to delineate the functionally important regions in aqueous-exposed cytoplasmic regions of the *E. coli* GlpG rhomboid.

EXPERIMENTAL PROCEDURES

Plasmids and Reagents. The C-terminally hexahistidine tagged *E. coli* GlpG rhomboid in a pET15b vector[38] was kindly provided by Christopher Koth's group of the Ontario Centre for Structural Genomics at the University of Toronto (Toronto, ON). This plasmid was used to create expression vectors for the C-terminal transmembrane domain consisting of residues 60−276 (TMD_{60}), 81−276 (TMD_{81}), and 91−276 (TMD_{91}). TMD_{60} and TMD_{81} were cloned into pET25b, and TMD_{91} was cloned into pET30a using primers synthesized by Integrated DNA Technologies, Inc. (Table 1 of the Supporting Information). All mutants were generated using the QuikChange site-directed mutagenesis protocol (Stratagene) and primers listed in Table 2 of the Supporting Information. All constructs were verified by sequencing performed at the Ontario Genomics Innovation Centre at the Ottawa Health Research Institute.

GlpG Expression and Purification. Expression vectors were transformed into *E. coli* C43(DE3) competent cells and grown at 37 °C in LB medium with 100 μg/mL ampicillin or 50 μg/mL kanamycin. When the optical density of the culture at 600 nm reached 0.5−0.7, the temperature was reduced to 16 °C and expression was induced with 1 mM isopropyl β-D-thiogalactopyranoside and allowed to proceed for 16−20 h. Detergent-solubilized protein was purified as described previously[17,38] with some modifications. Briefly, the bacterial pellet from 500 mL of culture was resuspended in 20 mM HEPES buffer (pH 7.3) containing 100 mM NaCl, 5 mM $MgCl_2$, 10% glycerol, and Complete EDTA-free protease inhibitor cocktail (Roche). Cells were lysed by sonication and centrifuged at 50000*g* for 1 h. The insoluble membrane fraction was resuspended in 50 mM HEPES buffer (pH 7.3) containing 1% (w/v) dodecyl maltoside (DDM) (Anatrace), 200 mM NaCl, 10% glycerol, 5 mM imidazole, and protease inhibitor cocktail for 1 h and then centrifuged for 30 min at 50000*g*. The DDM-solubilized protein in the supernatant was applied to a nickel affinity column equilibrated in the same buffer without detergent and then washed in 50 mM HEPES buffer (pH 7.3) containing 0.1% DDM, 500 mM NaCl, 10% glycerol, and 30 mM imidazole. A similar wash with 200 mM NaCl was performed prior to elution in 50 mM HEPES buffer (pH 7.3) containing 0.1% DDM, 200 mM NaCl, 10% glycerol, and 250 mM imidazole. Eluted protein was concentrated using a 30 kDa molecular mass cutoff ultracentrifugation device (Amicon Ultra) and then applied to a Superdex-200 size exclusion column using an AKTA FPLC system (GE Healthcare) equilibrated in 50 mM HEPES buffer (pH 7.3) containing 0.1% detergent, 200 mM NaCl, 10% glycerol, and 100 μM EDTA. Production of the TMD construct by limited proteolysis was performed as described previously[18] using trypsin, and the digest was reapplied to the size exclusion column to isolate the transmembrane domain. All samples were reapplied directly onto the size exclusion column to obtain a >90% pure protein sample as judged by Coomassie-stained sodium dodecyl sulfate−polyacrylamide gel electrophoresis (SDS−PAGE), with highly similar degrees of purity for truncation and point mutant samples (Figure 1 of the Supporting Information). Matrix-assisted laser desorption ionization time-of-flight mass spectrometry (MALDI-TOF MS) was used to analyze the full-length and trypsin-generated TMD sample using a Microflex MALDI-TOF mass spectrometer (Bruker) and the ultrathin layer method with α-cyano-4-hydroxycinnamic acid as the matrix.[39]

Determination of the CytD Structure. *E. coli* GlpG CytD (residues 1−61) was cloned into the pET30a vector between the NdeI and XhoI restriction sites to contain a C-terminal His_6 tag preceded by a Leu-Glu sequence. The CytD expression plasmid was transformed into BL21(DE3) cells, which were then grown in M9 containing 0.1% (w/v) ^{15}N-labeled ammonium chloride and 0.3% (w/v) glucose (U-^{13}C) as the sole nitrogen and carbon sources, respectively, as well as 50 μg/mL kanamycin. The bacterial pellet from a 1 L culture was resuspended in 25 mM phosphate buffer (pH 6.5) containing 150 mM NaCl, EDTA-free protease inhibitor cocktail (Roche), and 10 mM imidazole and lysed by sonication. Cell debris was centrifuged at 16000*g* for 20 min, and the CytD was purified by nickel affinity chromatography. Concentrated CytD fractions were subjected to size exclusion chromatography on a Superdex 75 column (GE Healthcare) equilibrated in phosphate buffer (pH 6.5) containing 150 mM NaCl and 100 μM EDTA. Concentrated samples for NMR analysis typically contained ∼1 mM CytD in 25 mM phosphate buffer (pH 6.5), 150 mM NaCl, and 10% D_2O.

All NMR spectra were recorded at 25 °C on a Varian Inova 500 spectrometer equipped with a triple-resonance pulsed field gradient probe at the University of Ottawa NMR Facility. ^{15}N HSQC, ^{13}C HSQC, HNCO, HNCA, HNCACB, HBHA(CO)-NH, HN(CO)CA, HCCH-TOCSY, HCCH-COSY, ^{13}C NOESY-HSQC, and ^{15}N NOESY-HSQC experiments were used to determine the structure.[40] Data were processed with NMRPipe[41] and analyzed with NMRView.[42] NOE distance restraints and backbone dihedral angles derived from TALOS[43] were used in the torsion angle dynamics program CYANA version 2.1,[44] which performed automatic NOE assignment to calculate 200 conformers. The 20 lowest-energy structures from the final round of CYANA were individually refined in explicit

solvent[45] using XPLOR-NIH[46,47] and scripts available from ftp://ftp.pasteur.fr/pub/BIS/linge/. Subsequently, the quality of the solvent-refined structures was validated by using AQUA, PROCHECK,[48,49] and WHAT IF.[50] Structural statistics are listed in Table 3 of the Supporting Information. Chemical shift assignments and structure coordinates were deposited in the Biological Magnetic Resonance Data Bank (entry 17720) and the Protein Data Bank (PDB) (entry 2LEP), respectively.

Rhomboid Protease Assay Using Fluorogenic Casein. After the protein concentration had been determined using the BCA assay,[51] wild-type, truncated, and mutant GlpG were assayed for activity using BODIPY-labeled casein (Invitrogen). This rhomboid assay was based on previously described protocols,[18] where 5 μg of BODIPY FL casein was incubated with 0.8 μM GlpG in 50 mM HEPES buffer (pH 7.3) containing 0.1% detergent, 200 mM NaCl, 10% glycerol, and 100 μM EDTA at 37 °C. Fluorescence excitation of a 200 μL volume was induced at 485 nm and emission monitored at 530 nm using a SpectraMax 5 microplate reader (Molecular Devices) in the top-reading mode. All samples were assayed in duplicate against a buffer blank, with assays on each mutant being repeated with at least two different purified samples. Specific activities were calculated using the slope of relative fluorescence units (rfu) over 30 min after a 10 min equilibration period.

Active Rhomboid Labeling with FP-PEG-Rhodamine. Purified rhomboid (10 μg) was incubated in the dark with 10 nM FP-PEG-rhodamine (from a 0.1 μM stock in DMSO; final DMSO concentration of 0.2%) for 2 min at 37 °C, and the reaction was quenched by precipitating the proteome with 5 volumes of ice-cold acetone to remove unreacted probe. The crude membrane extract in 1% DDM (40 μg of total protein at 1 mg/mL) was incubated for 1 h with FP-PEG-rhodamine using the same conditions that were used for purified rhomboid. The precipitated proteins were subjected to SDS–PAGE separation on a 15% gel (1.5 mm thickness) at 100 V. The gels were scanned for fluorescence using the FMBIO III instrument (Hitachi Solutions Ltd., Tsurumi-ku Yokohama, Japan) to visualize the active protein. The amount of FP-PEG-rhodamine labeling in crude membrane extracts was measured by integrating fluorescent band intensities and subtracting background intensity from these measurements. FP-PEG-rhodamine labeling was normalized for differential protein expression using relative intensities measured via Coomassie-stained SDS–PAGE. All labeling reactions were performed in duplicate or triplicate.

RESULTS

Isolation and Activity of the TMD Core. To confirm the functional importance of the GlpG cytoplasmic N-terminal sequence, we performed limited proteolysis with trypsin to isolate the TMD core.[20] Similar to previous observations using fluorogenic casein as a rhomboid substrate,[18] this TMD sample displayed roughly half the specific activity of the full-length GlpG over the range of substrate concentrations tested (Figure 2A of the Supporting Information). Both full-length and TMD samples gave rise to Michaelis–Menten kinetic profiles, with the maximal velocity (V_{max}) for the TMD being roughly half that of the full-length protein, while the Michaelis constant (K_m) was not altered (Figure 2B of the Supporting Information).

GlpG Residues 1–61 Form a Structured Domain. Solution NMR previously performed on a fragment from the N-terminus of the GlpG-like rhomboid from *P. aeruginosa* showed that the first ~70 residues form a compact $\alpha\beta$ structure, with the remaining ~20 cytoplasmic residues being largely unstructured.[52] Given the low degree of sequence homology with the N-terminus of the *E. coli* GlpG rhomboid (25% identical sequence for residues 1–91), we determined the structure of the analogous region of the *E. coli* homologue to inform our investigations on potential functional influences exerted by this domain. As shown in Figure 1, residues 1–61 from *E. coli* GlpG, called the cytoplasmic domain (CytD), form a compact structure consisting of a three-stranded β-sheet, (β1, residues 2–7; β2, residues 27–30; β3, residues 35–39) and two α-helices (α1, residues 10–22; α2, residues 42–57) packed against the hydrophobic side of the sheet. The α-helices interact extensively with each other and the β-sheet via a conserved cluster of hydrophobic and aromatic residues that form the core. This is different from the *Pseudomonas* structure that shows almost orthogonal relative positioning of the two helices with respect to each other, along with less extensive interactions between these helices, giving rise to a relatively high Cα rmsd between the two structures [6.45 Å (Figure 3B of the Supporting Information)]. Aside from this hydrophobic core, regions of the cytoplasmic domain showing the highest degree of sequence conservation among homologues from *Enterobacteriaceae* species map to the surface-exposed surface of α1 (Figure 1A), suggesting a potential role for inter- or intramolecular interactions. Consequently, mutations were introduced at two sites in this conserved helix (i.e., R11A and D18A), as well as the conserved Asn preceding this helix (N9A) and Trp in the central part of the β-sheet (W38A), to allow evaluation of the functional role of these residues.

Interactions of the TMD Cytoplasmic Face. To determine if interactions between the CytD and cytoplasmic face of the TMD could account for differences in activity observed between full-length and TMD GlpG, mutations were introduced at the conserved solvent-exposed sites in the CytD described above, or conserved residues in the cytoplasmic side of the TMD (Figure 1 and Table 4 of the Supporting Information). In our initial screens, proteolysis activity was assessed with the same casein-based assay used for the TMD. This assay showed that mutants E216A and R227A had reduced activity compared to that of wild-type GlpG (Figure 1C), with peptide hydrolysis rates being similar to that of the active site serine knockout S201A. A small but significant decrease in activity was also observed for K167A, D218A, and Y224A, which showed 30–40% lower activity than wild-type GlpG. In contrast, mutations made in the CytD (i.e., N9A, R11A, D18A, and W38A) did not significantly alter polypeptide cleavage rates, suggesting that these sites are not critical for proteolysis activity. Furthermore, the presumably destabilizing introduction of a negatively charged residue into the hydrophobic core of the CytD (F55D) did not have an effect on protease activity, suggesting that the CytD does not play a role in modulating catalysis (Figure 1C).

To delineate more precisely the functionally important region of the N-terminal sequence that gave rise to the observed reduction in TMD activity, we made three truncation mutants: TMD_{60} (GlpG residues 60–276) that lacks only the CytD, TMD_{91} (residues 91–276) that omits all N-terminal residues not observed in the GlpG TMD X-ray structures, and TMD_{81} (residues 81–276) that is slightly longer than the fragment obtained after chymotrypsin digestion.[18] As shown in Figure 1C, two constructs lacking a substantial portion of the

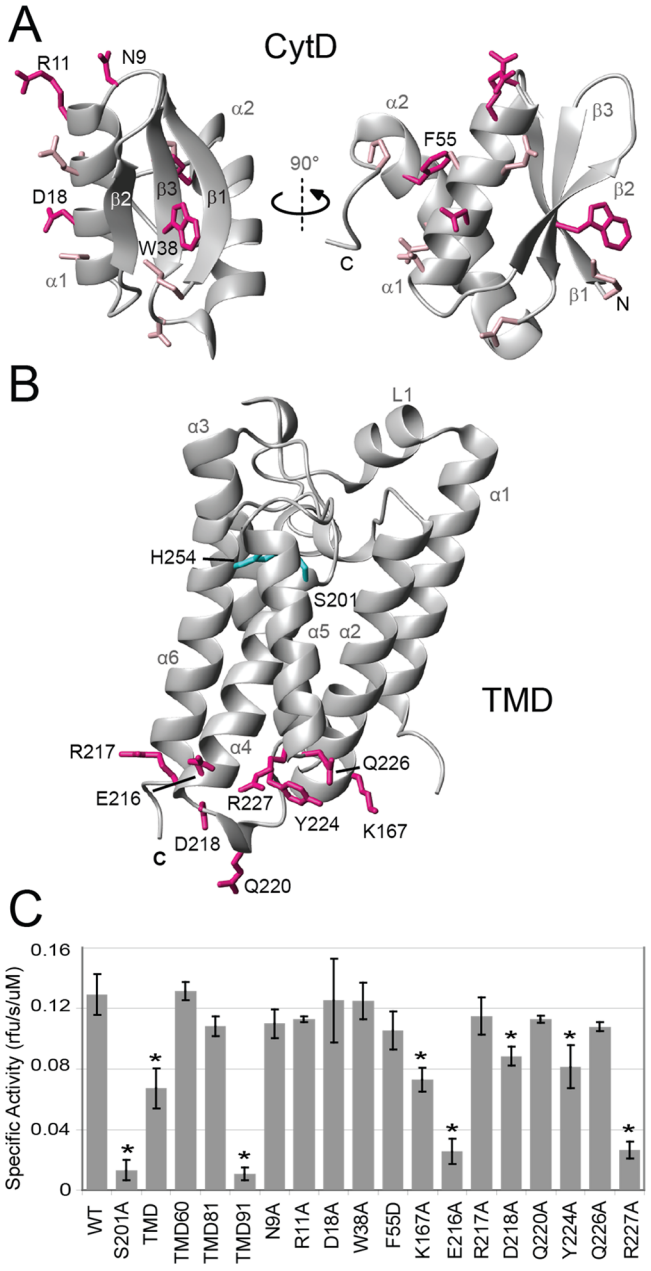

Figure 1. Identification of functionally important residues at the cytoplasmic face of the TMD. (A) Solution NMR structure of *E. coli* GlpG CytD. Surface-exposed residues showing the highest degree of sequence conservation among homologues from *Enterobacteriaceae* species are indicated (Table 4 of the Supporting Information), with residues that were mutated to alanine highlighted in dark pink. (B) Location of residues that were mutated in the GlpG TMD structure (PDB entry 2IC8[18]), highlighted in pink, and active site residues, highlighted in blue. (C) Specific activities using fluorogenic casein as the substrate for trypsin-isolated TMD, the wild type and indicated mutants of GlpG. Activities that were significantly lower than that of the wild type (WT) are identified by asterisks ($p < 0.05$).

N-terminal sequence (TMD_{60} and TMD_{81}) displayed the same level of activity as the full-length protein, indicating that this part of the cytoplasmic region is not responsible for the reduction in activity observed with trypsin-generated TMD. In contrast, TMD_{91} was essentially inactive, although GlpG X-ray structures begin at E91 or later in the sequence.[18−24] This suggested that only 10 additional amino acids N-terminal to the first TM helix are required for maintaining an active state for the TMD.

Although TMD_{91} exhibited no activity in the casein assay, the TMD product of limited trypsin proteolysis did show significant activity, albeit at lower levels than the full-length protein. However, the loop connecting the cytoplasmic domain to the TMD has multiple potential cleavage sites that could produce a mixture of active and inactive digestion products. To evaluate the homogeneity of the purified trypsin digest, MALDI-TOF MS was performed on a purified TMD produced by trypsinolysis (Figure 4 of the Supporting Information). These spectra showed that this sample is comprised of a mixture of cleavage products and is consistent with the decrease in V_{max} and unchanged K_m that were observed relative to those of the full-length protein, because the trypsin digest produced a mix of active and inactive TMD.

One of the drawbacks to the fluorogenic substrate used in this study was the requirement for purified rhomboid samples to be generated for each mutant, with high background activity from other proteases preventing analysis of crude membrane extracts (data not shown). More recently, a similar type of fluorescence-based assay was developed using a water-soluble fragment of a known rhomboid substrate sequence, although susceptibility to other proteases was also retained in its design.[53] Consequently, these assays cannot be used to assess the function of rhomboids or their mutants in the more stabilizing environment of the lipid membrane. However, the use of purified rhomboid samples can overemphasize the influence of mutations on protease function because interactions with the native lipid tend to be supplanted by detergent interactions during purification, providing a less stabilizing environment (for reviews, see refs 54−58). This may be particularly significant for the rhomboid, because interactions with the surrounding lipid have been proposed to be important for membrane positioning effects,[59−61] and discrepancies between rhomboid activities in detergents versus lipid membranes have previously been reported.[6,38,60,62,63] For these reasons, we have investigated the ability of the ABPP approach to avoid these problems by allowing rhomboid active sites to be specifically labeled from crude membrane preparations prior to separation from the rest of the proteomic sample using SDS−PAGE (Figure 2B).

Active Site Labeling of Purified Rhomboid Protease. To evaluate the utility of an ABPP approach to assay rhomboid function, we used a rhodamine-tagged fluorophosphonate [FP-PEG-rhodamine (Figure 2A)] ABP known to be specific for serine hydrolases.[64] This type of probe has been used in ABPP of soluble serine hydrolases[65,66] as well as the membrane-associated carboxylesterase 1.[67] Although diisopropyl fluorophosphonate (DFP) has previously been described as a weak rhomboid inhibitor (in the micromolar range),[24,68] we found that the FP-PEG-rhodamine ABP was able to label GlpG at a concentration of 10 nM (Figures 2C and 3A), where it is expected to enter the rhomboid active site from the aqueous phase. The GlpG crystal structure of the DFP adduct[24] suggests that the bulky PEG-rhodamine from our probe should project out of the binding pocket into the solvent, making the probe compatible with the membrane-submerged structural features of the active site. Covalent modification of purified GlpG by the FP-PEG-rhodamine was found to be specific for activity, as wild-type GlpG was labeled by the ABP while the active site serine mutant S201A was not (Figure 2C). Moreover, ABPP results with the truncation mutants were consistent with those

dx.doi.org/10.1021/bi301087c | *Biochemistry* 2012, 51, 7794−7803

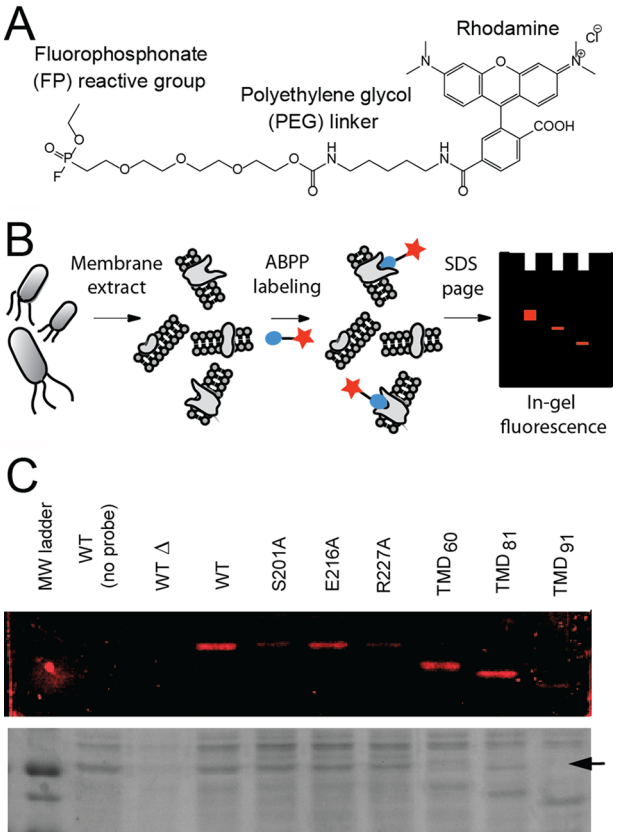

Figure 2. Rhomboid active site labeling using a fluorophosphonate fluorescent probe. (A) Chemical structure of the fluorophosphonate probe (FP-PEG-rhodamine). (B) Scheme for activity-based profiling of rhomboid protease activity. (C) Fluorescent probe labeling of purified wild-type, mutant, and truncated versions of the GlpG rhomboid protease. Visualization was done by rhodamine fluorescence (top), followed by silver stain (below). Rhomboid samples were labeled for 2 min in 50 mM HEPES (pH 7.3), 0.1% dodecyl maltoside (DDM), 200 mM NaCl, 10% glycerol, and 100 μM EDTA with 10 nM FP-PEG-rhodamine (from a 0.1 μM stock in DMSO; final DMSO concentration of 0.2%) before ice-cold acetone precipitation was used to isolate the protein fraction from the unreacted probe. The expected position for full-length GlpG and mutants is indicated by the arrow. WT Δ refers to a purified wild-type sample that has been heat-denatured by being exposed to 100 °C for 10 min.

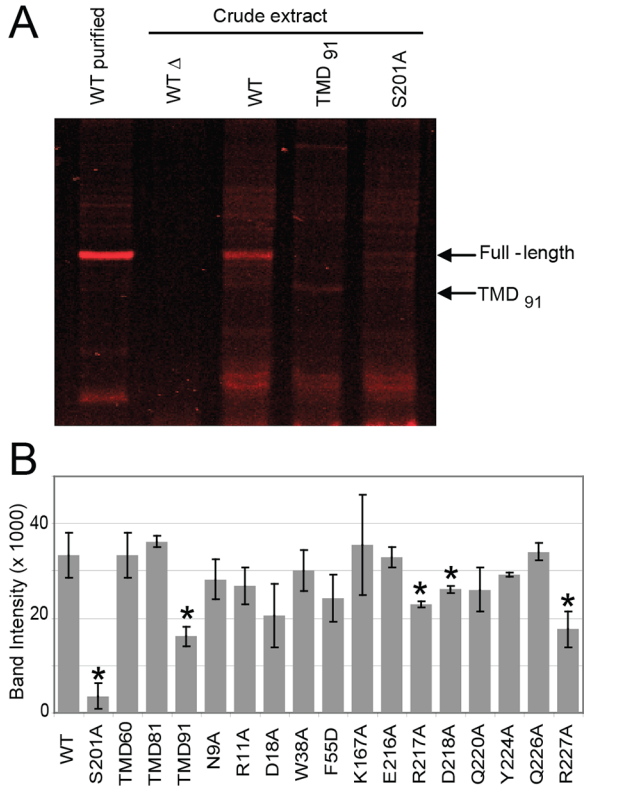

Figure 3. Identification of functionally important residues when the rhomboid is isolated in crude membranes. (A) Fluorescent probe labeling of wild-type, mutant, and truncated GlpG rhomboid protease in crude membrane proteomes. Membrane extracts were incubated with the probe for 1 h, and 40 μg of total protein was loaded onto the gel. (B) Expression-normalized fluorescence band intensities from FP-PEG-rhodamine-labeled crude membrane extracts measured for TMD truncation and full-length wild-type and mutant rhomboid samples. Intensities were normalized for variances in expression with significant differences in labeling from that of the wild type ($p < 0.05$) identified by asterisks.

obtained using the fluorogenic protein substrate (Figures 1C and 2C), with only TMD_{91} showing a significant reduction in the level of labeling. These results demonstrate that FP-PEG-rhodamine is a suitable ABP for GlpG.

Active Site Labeling of the Rhomboid in Crude Membrane Extracts. To test the ability of FP-PEG-rhodamine to assay GlpG function in a proteomic sample, crude membrane fractions isolated from bacteria expressing wild-type or mutant GlpG samples were suspended in the same detergent normally used for GlpG purification. As shown in Figure 3A, a band with significantly higher fluorescence readings over background levels was observed at the molecular weight expected for full-length GlpG that was not seen for the S201A mutant. Moreover, it was possible to quantitate the relative extent of labeling after normalizing for the amount of expressed protein loaded in each sample. Using this approach, a quantitative measure of ABPP-based activity could be obtained for all mutants in cellular membrane extracts (Figure 3B). In general, the effect of mutations on rhomboid activity was less severe than that observed in purified samples, a result that is not altogether unexpected in the more stabilizing environment of the lipid bilayer. For example, labeling of TMD_{91} is almost completely abrogated in purified samples (Figure 2C), whereas it is reduced by only ~50% when the experiment was performed in crude membrane extracts (Figure 3). This was not the case for the catalytic serine knockout mutant S201A, which showed no labeling in crude membrane extracts or purified samples in detergent. The difference between detergent-solubilized and crude membrane activities observed for samples such as TMD_{91} therefore suggests that these mutants were destabilized by the detergent conditions to a greater extent than the wild-type enzyme.

There were some mutants with less functionality in the casein assay that also showed reduced levels of active site labeling in crude membrane extracts, namely, D218A, R227A, and TMD_{91}. Interestingly, R217A also showed a similarly small decrease in the level of labeling, even though it was fully active against the casein substrate. While the exact mechanism behind this difference is not known, it appears that the E216–D218 stretch of amino acids at the end helix 4 may sense changes in the local environment in a way that affects the structure of the active site. This helix contains the precisely positioned active

dx.doi.org/10.1021/bi301087c | Biochemistry 2012, 51, 7794–7803

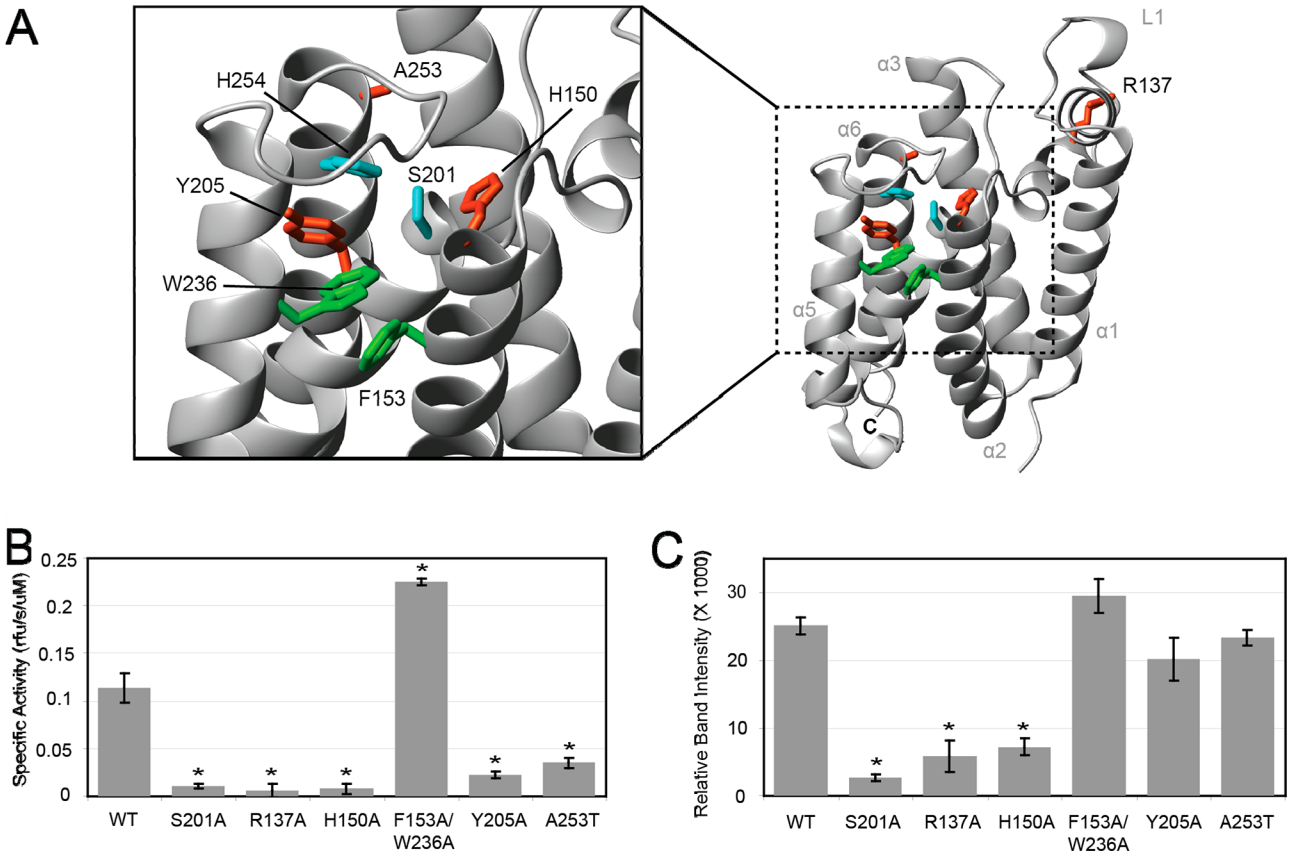

Figure 4. Changes in the GlpG active state detected through active site labeling. (A) Location of residues that were mutated in the GlpG TMD structure (PDB entry 2IC8[18]). Mutations expected to decrease rhomboid activity are colored orange, and mutations comprising the double mutant expected to increase rhomboid activity are colored green. (B) Specific activities using fluorogenic casein as the substrate for the indicated mutants of GlpG. Specific activities that were significantly different than that of the wild type are identified by asterisks ($p < 0.05$). (C) Fluorescent probe labeling of wild-type and mutant GlpG in crude membrane proteomes. Expression-normalized fluorescence band intensities that show significant differences in labeling vs that of the wild type ($p < 0.05$) are identified by asterisks.

site serine at its N-terminal side, which could be altered by these mutations (Figure 5B of the Supporting Information).

Complementarity of ABPP- and Proteolysis-Based Assays. An interesting feature of the FP-PEG-rhodamine ABP was highlighted by the apparent discrepancy in results for mutant E216A, which had a greatly reduced ability to hydrolyze a polypeptide substrate yet still underwent efficient labeling by the ABP, even after purification in detergent (Figures 1C and 2C). These two different outcomes for the same mutant suggest that the ABPP approach can also be used to distinguish between mutations that alter the catalytic status of active site residues, versus those that disrupt proteolytic activity by some other mechanism, such as inhibition of substrate entry. To test this idea, an additional set of mutations previously shown to inactivate the rhomboid through various mechanisms was evaluated using the ABPP and casein assays. These include R137A,[6,60−62] H150A,[60,62] Y205A,[60,62] and A253T,[22] mutations expected to disrupt L1 loop structure, oxyanion binding, catalytic serine activation, and S1 pocket specificity, respectively. As shown in Figure 4, these mutants showed significantly lower activity against casein, as was previously observed in studies using TMD-based substrates. However, as expected, only those mutants that are known to alter the catalytic integrity of active site residues were impaired in FP-PEG-rhodamine labeling, namely, R137A and H150A (Figure 4C and Figure 6 of the Supporting Information). Specifically, Arg137 has a critical structural role,[69] with the mutation to alanine disrupting the stability, and likely the structure, of the active site. Similarly, while the stability of H150A is the same as that of the wild-type protein,[69] this mutant lacks a key residue required for stabilization of the oxyanion in the transition state. Therefore, the inability of either of these mutants to undergo reaction with FP-PEG-rhodamine confirms its utility as a probe of active site structure and catalytic integrity.

Other mutants showed differential activity as evaluated by the proteolysis assay versus the ABPP method. One example is that of the mutant A253T, which is not expected to alter the activation status of catalytically important residues. Instead, entry of a substrate polypeptide into the active site should be inhibited because Ala253 sits at the mouth of the P1 pocket that binds a bulky hydrophobic side chain without altering the activation status of catalytic residues.[22] This is consistent with the observed impairment of polypeptide hydrolysis but robust labeling by FP-PEG-rhodamine. Additional confirmation that ABPP together with proteolysis-based assays of activity can identify mutants that alter substrate entry or binding is provided by our results with the F153A/W236A double mutant. The loss of gating residues proposed to line the substrate entry site between TM helices 2 and 5 has been shown to increase the rate of TM substrate hydrolysis,[60,62] an outcome that we also obtained using the casein substrate (Figure 4B). No difference in labeling by FP-PEG-rhodamine was observed for this mutant, confirming that this increase in

dx.doi.org/10.1021/bi301087c | Biochemistry 2012, 51, 7794−7803

activity does not come about because of an increase in the catalytic efficiency of active site residues.

One unexpected result arising from this series of mutants was the robust labeling seen for the proteolytically inactive Y205A mutant, even though this residue is thought to play a role in fixing the orientation of the imidazole ring from His254 that is required to activate the catalytic serine.[18,60,62] Our results indicate that the nucleophilic state of this Ser is preserved in the Y205A mutant, suggesting that this residue may play a role in proteolysis different from that previously proposed. In fact, a series of crystal structures with GlpG covalently modified by fluorophosphonate- or isocoumarin-based inhibitors shows a reorientation of this side chain that appears to be coupled with changes in the orientation of gating residue Trp236 in TM5.[24] In the apo structure, the Trp236 indole ring occupies a region of the active site that has been proposed to block the putative binding pocket for the substrate P2′ side chain.[22] Our results suggest that the loss of Tyr205 may lead to a structural change in this region that potentially prevents the reorientation of Trp236 that is required for peptide binding[22] but would not be needed for reaction with a fluorophosphonate inhibitor.[24]

DISCUSSION

Previous work on the *Pseudomonas* GlpG-like rhomboid had suggested that the cytoplasmic and transmembrane domains might interact in a way to enhance activity.[17] However, the truncation mutants of *E. coli* GlpG detailed in this study revealed that removal of the structured CytD, as well as most of the N-terminus up to Arg81, had no significant effect on protease activity against casein or reactivity of the active site with FP-PEG-rhodamine. Nonetheless, the conservation of this domain in the GlpG family, along with the identification of a conserved patch of surface-exposed residues that line one side of α1, argues for a functionally important role for this domain that has yet to be discovered. A potential clue may be provided by the results of a structural homology search[70,71] showing that the CytD structure is highly similar to the that of sporulation-related domain (SPOR, Pfam accession number 05036[72]) found in the bacterial cell division protein FtsN,[73] with the exception that the SPOR domain typically has an extra β-strand at the C-terminus (Figure 7 of the Supporting Information). This domain has been shown to act as a binding module, with its most well-characterized role being that of a peptidoglycan-binding domain required for localization to the cytokinetic septum during bacterial cell division.[74−76] An intriguing link between the SPOR domain and GlpG is provided by the sole phenotype that has been identified in the *E. coli* GlpG knockout. This strain showed a decreased susceptibility to an antibiotic that binds the peptidoglycan synthase required for the last stage of bacterial cell wall synthesis in cell division, but not other antibiotics that act by different mechanisms,[77] a phenotype that is strikingly similar to that of an FtsN-depleted strain of *E. coli*.[78] Although these observations may invite speculation about a role for GlpG in some aspect of divisome assembly, the true function of the CytD will nonetheless remain a mystery until the physiological substrate is identified.

While our results show that the CytD is not required for proteolytic function in GlpG, this is the first study to implicate a functional role for residues 81−90, an aqueous-exposed segment that is a few residues from the N-terminus of TM1. There is no structural information yet available for this part of the protein, with most structures determined using protease-generated fragments containing residues 91−270[18−24] that show TM1 starting at residue 95, with the four preceding residues being in a more extended conformation. Only one GlpG structure used a slightly longer construct starting at residue 87, although no electron density was fit for residues 87−90.[19] The helix-initiating role of Pro95[79] in TM1 makes it unlikely that the shorter constructs prematurely truncate this TM helix, particularly given the high degree of structural similarity for the resolved structure preceding TM1 over a range of crystallization conditions.

Sequence analysis of residues 81−90 provides a potential clue into the structure of this segment, with a prediction for amphipathic helix formation[80] for residues Phe85−Glu-91 that is conserved throughout the rhomboid family (Figure 8 of the Supporting Information). This could facilitate a direct interaction between this helix and the lipid bilayer for additional membrane positioning purposes. Alternatively, this short segment may be involved in interactions with functionally important residues from the TMD, such as those identified in this study. In particular, all X-ray structures that were able to resolve residue 91 show it in the proximity of Lys167 and Tyr224, residues that may serve as an interaction site with this pre-TM1 segment.

The functional importance of the pre-TM1 segment is particularly intriguing given the recent identification of an inactivating cleavage event that occurs in the mitochondrial homologue presenilin-associated rhomboid-like (PARL) protein.[81] The mitochondrial rhomboid family is characterized by an additional N-terminal TM helix[82] (sometimes called TM A) that is eliminated by cleavage of a sequence preceding TM1 with weak homology to the GlpG pre-TM1 sequence (Figure 9A of the Supporting Information). While it has been proposed that the loss of this extra TM helix is responsible for inactivation, our results also raise the possibility that the loss of the pre-TM1 sequence may be inactivating for PARL family proteins.

In addition to the pre-TM1 segment, this is also the first study to identify a functional role for Arg227 on TM5, which appears to project out into the lipid phase in all published rhomboid structures.[18−24] While it is not yet possible to identify the mechanism by which the R227A mutation alters the catalytic status of active site residues, there is some evidence to suggest that this side chain participates in specific interactions with lipid or detergent molecules. For example, a recent crystal structure for GlpG in dimyristoylphosphatidylcholine (DMPC)/CHAPS bicelles shows a DMPC molecule bound in the interface between TM2 and TM5, with the choline group in the proximity of the Arg227 side chain.[23] Molecular dynamics simulations of GlpG in 1-palmitoyl-2-oleoylphosphatidylcholine (POPC) and 1-palmitoyl-2-oleoylphosphatidylethanolamine (POPE) bilayers also show hydrogen bonding interactions involving lipid headgroups and the Arg227 side chain.[59] These same simulations revealed functional coupling among TM5, L1, and the active site with perturbations in TM5 affecting the local structure and GlpG orientation in the membrane. It is tempting to speculate that loss of lipid binding capabilities by this residue could change the conformational dynamics of TM5 and other dynamically coupled parts of the protein to alter its function. This not only would explain the reduction in activity for the R227A mutant but also might provide a mechanism for previous observations that different lipid environments promote various levels of rhomboid activity.[68]

CONCLUSION

In summary, we demonstrate that ABPP can effectively examine the activity of rhomboid proteases that are present in crude lipid extracts isolated from *E. coli*. When used in combination with protease-based assays of rhomboid function, efficiencies of labeling by the FP-PEG-rhodamine probe can distinguish between mutations that disrupt the catalytic integrity of the active site and those that alter substrate binding. Using this approach, we identify an N-terminal sequence that is critical for maintaining a catalytically competent state for the *E. coli* GlpG rhomboid, even under the more stabilizing conditions provided by solubilized membranes. Future structural studies of GlpG that include this critical N-terminal sequence will be required to determine how these residues influence the active site in both micelle and membrane environments, and if it functions through membrane positioning and/or interactions with the TMD cytoplasmic face. We also identify Arg227 as a functionally important lipid-facing residue, suggesting a role for specific protein−lipid interactions. These functional insights should be relevant for future inhibitor development, particularly given the emergence of the rhomboid as a potential target in parasites that rely on rhomboid function for pathogenicity.[4,83,84] Inhibition of active site labeling by the FP-PEG-rhodamine probe used in this study may provide a convenient monitor for the identification of potential leads in these future investigations.

ASSOCIATED CONTENT

Supporting Information

Additional observations. This material is available free of charge via the Internet at http://pubs.acs.org.

AUTHOR INFORMATION

Corresponding Author

*E-mail: john.pezacki@nrc.ca (J.P.P.) or ngoto@uottawa.ca (N.K.G.).

Funding

N.K.G. and J.P.P. thank the Natural Sciences and Engineering Council of Canada (NSERC) for funding.

Notes

The authors declare no competing financial interest.

ACKNOWLEDGMENTS

We thank Shuqiong Lin for synthesizing the FP-PEG-rhodamine probe and Dr. Benjamin Cravatt from the Scripps Research Institute for helpful discussions about this work.

ABBREVIATIONS

ABP, activity-based probe; ABPP, activity-based protein profiling; BCA, bicinchoninic acid; CHAPS, 3-[(3-cholamidopropyl)dimethylammonio]-1-propanesulfonate; CytD, cytoplasmic domain; DDM, dodecyl maltoside; DFP, diisopropyl fluorophosphonate; DMPC, dimyristoylphosphatidylcholine; PARL, presenilin-associated rhomboid-like; POPC, 1-palmitoyl-2-oleoylphosphatidylcholine; POPE, 1-palmitoyl-2-oleoylphosphatidylethanolamine; TMD, transmembrane domain.

REFERENCES

(1) Brown, M. S., Ye, J., Rawson, R. B., and Goldstein, J. L. (2000) Regulated intramembrane proteolysis: A control mechanism conserved from bacteria to humans. *Cell 100*, 391−398.

(2) Koonin, E. V., Makarova, K. S., Rogozin, I. B., Davidovic, L., Letellier, M. C., and Pellegrini, L. (2003) The rhomboids: A nearly ubiquitous family of intramembrane serine proteases that probably evolved by multiple ancient horizontal gene transfers. *Genome Biol. 4*, R19.

(3) Urban, S., and Dickey, S. W. (2011) The rhomboid protease family: A decade of progress on function and mechanism. *Genome Biol. 12*, 231.

(4) Freeman, M. (2008) Rhomboid proteases and their biological functions. *Annu. Rev. Genet. 42*, 191−210.

(5) Adrain, C., Strisovsky, K., Zettl, M., Hu, L., Lemberg, M. K., and Freeman, M. (2011) Mammalian EGF receptor activation by the rhomboid protease RHBDL2. *EMBO Rep. 12*, 421−427.

(6) Urban, S., Lee, J. R., and Freeman, M. (2001) *Drosophila* Rhomboid-1 defines a family of putative intramembrane serine proteases. *Cell 107*, 173−182.

(7) Herlan, M., Vogel, F., Bornhovd, C., Neupert, W., and Reichert, A. S. (2003) Processing of Mgm1 by the rhomboid-type protease Pcp1 is required for maintenance of mitochondrial morphology and of mitochondrial DNA. *J. Biol. Chem. 278*, 27781−27788.

(8) McQuibban, G. A., Saurya, S., and Freeman, M. (2003) Mitochondrial membrane remodelling regulated by a conserved rhomboid protease. *Nature 423*, 537−541.

(9) Cipolat, S., Rudka, T., Hartmann, D., Costa, V., Serneels, L., Craessaerts, K., Metzger, K., Frezza, C., Annaert, W., D'Adamio, L., Derks, C., Dejaegere, T., Pellegrini, L., D'Hooge, R., Scorrano, L., and De Strooper, B. (2006) Mitochondrial rhomboid PARL regulates cytochrome c release during apoptosis via OPA1-dependent cristae remodeling. *Cell 126*, 163−175.

(10) Chao, J. R., Parganas, E., Boyd, K., Hong, C. Y., Opferman, J. T., and Ihle, J. N. (2008) Hax1-mediated processing of HtrA2 by Parl allows survival of lymphocytes and neurons. *Nature 452*, 98−102.

(11) Stevenson, L. G., Strisovsky, K., Clemmer, K. M., Bhatt, S., Freeman, M., and Rather, P. N. (2007) Rhomboid protease AarA mediates quorum-sensing in *Providencia stuartii* by activating TatA of the twin-arginine translocase. *Proc. Natl. Acad. Sci. U.S.A. 104*, 1003−1008.

(12) Brossier, F., Jewett, T. J., Sibley, L. D., and Urban, S. (2005) A spatially localized rhomboid protease cleaves cell surface adhesins essential for invasion by Toxoplasma. *Proc. Natl. Acad. Sci. U.S.A. 102*, 4146−4151.

(13) Baxt, L. A., Baker, R. P., Singh, U., and Urban, S. (2008) An *Entamoeba histolytica* rhomboid protease with atypical specificity cleaves a surface lectin involved in phagocytosis and immune evasion. *Genes Dev. 22*, 1636−1646.

(14) Urban, S. (2010) Taking the plunge: Integrating structural, enzymatic and computational insights into a unified model for membrane-immersed rhomboid proteolysis. *Biochem. J. 425*, 501−512.

(15) Urban, S., and Shi, Y. (2008) Core principles of intramembrane proteolysis: Comparison of rhomboid and site-2 family proteases. *Curr. Opin. Struct. Biol. 18*, 432−441.

(16) Lohi, O., Urban, S., and Freeman, M. (2004) Diverse substrate recognition mechanisms for rhomboids; Thrombomodulin is cleaved by mammalian rhomboids. *Curr. Biol. 14*, 236−241.

(17) Sherratt, A. R., Braganza, M. V., Nguyen, E., Ducat, T., and Goto, N. K. (2009) Insights into the effect of detergents on the full-length rhomboid protease from *Pseudomonas aeruginosa* and its cytosolic domain. *Biochim. Biophys. Acta 1788*, 2444−2453.

(18) Wang, Y., Zhang, Y., and Ha, Y. (2006) Crystal structure of a rhomboid family intramembrane protease. *Nature 444*, 179−180.

(19) Wu, Z., Yan, N., Feng, L., Oberstein, A., Yan, H., Baker, R. P., Gu, L., Jeffrey, P. D., Urban, S., and Shi, Y. (2006) Structural analysis of a rhomboid family intramembrane protease reveals a gating mechanism for substrate entry. *Nat. Struct. Mol. Biol. 13*, 1084−1091.

(20) Ben-Shem, A., Fass, D., and Bibi, E. (2007) Structural basis for intramembrane proteolysis by rhomboid serine proteases. *Proc. Natl. Acad. Sci. U.S.A. 104*, 462−466.

(21) Wang, Y., and Ha, Y. (2007) Open-cap conformation of intramembrane protease GlpG. *Proc. Natl. Acad. Sci. U.S.A. 104*, 2098−2102.
(22) Vinothkumar, K. R., Strisovsky, K., Andreeva, A., Christova, Y., Verhelst, S., and Freeman, M. (2010) The structural basis for catalysis and substrate specificity of a rhomboid protease. *EMBO J. 29*, 3797−3809.
(23) Vinothkumar, K. R. (2011) Structure of rhomboid protease in a lipid environment. *J. Mol. Biol. 407*, 232−247.
(24) Xue, Y., and Ha, Y. (2012) The catalytic mechanism of rhomboid protease GlpG probed by 3,4-dichloroisocoumarin and diisopropyl fluorophosphonate. *J. Biol. Chem. 287*, 3099−3107.
(25) Puri, A. W., and Bogyo, M. (2009) Using small molecules to dissect mechanisms of microbial pathogenesis. *ACS Chem. Biol. 4*, 603−616.
(26) Cravatt, B. F., Wright, A. T., and Kozarich, J. W. (2008) Activity-based protein profiling: From enzyme chemistry to proteomic chemistry. *Annu. Rev. Biochem. 77*, 383−414.
(27) Blais, D. R., Nasheri, N., McKay, C. S., Legault, M. C., and Pezacki, J. P. (2012) Activity-based protein profiling of host-virus interactions. *Trends Biotechnol. 30*, 89−99.
(28) Fonovic, M., and Bogyo, M. (2008) Activity-based probes as a tool for functional proteomic analysis of proteases. *Expert Rev. Proteomics 5*, 721−730.
(29) Uttamchandani, M., Li, J., Sun, H., and Yao, S. Q. (2008) Activity-based protein profiling: New developments and directions in functional proteomics. *ChemBioChem 9*, 667−675.
(30) Bachovchin, D. A., Ji, T., Li, W., Simon, G. M., Blankman, J. L., Adibekian, A., Hoover, H., Niessen, S., and Cravatt, B. F. (2010) Superfamily-wide portrait of serine hydrolase inhibition achieved by library-versus-library screening. *Proc. Natl. Acad. Sci. U.S.A. 107*, 20941−20946.
(31) Jessani, N., Humphrey, M., McDonald, W. H., Niessen, S., Masuda, K., Gangadharan, B., Yates, J. R., Mueller, B. M., and Cravatt, B. F. (2004) Carcinoma and stromal enzyme activity profiles associated with breast tumor growth in vivo. *Proc. Natl. Acad. Sci. U.S.A. 101*, 13756−13761.
(32) Kaschani, F., Gu, C., Niessen, S., Hoover, H., Cravatt, B. F., and van der Hoorn, R. A. L. (2009) Diversity of serine hydrolase activities of unchallenged and botrytis-infected *Arabidopsis thaliana*. *Mol. Cell. Proteomics 8*, 1082−1093.
(33) Kidd, D., Liu, Y. S., and Cravatt, B. F. (2001) Profiling serine hydrolase activities in complex proteomes. *Biochemistry 40*, 4005−4015.
(34) Liu, Y. S., Patricelli, M. P., and Cravatt, B. F. (1999) Activity-based protein profiling: The serine hydrolases. *Proc. Natl. Acad. Sci. U.S.A. 96*, 14694−14699.
(35) Chang, J. W., Nomura, D. K., and Cravatt, B. F. (2011) A Potent and Selective Inhibitor of KIAA1363/AADACL1 that Impairs Prostate Cancer Pathogenesis. *Chem. Biol. 18*, 476−484.
(36) Nomura, D. K., Leungt, D., Chiang, K. P., Quistad, G. B., Cravatt, B. F., and Casida, J. E. (2005) A brain detoxifying enzyme for organophosphorus nerve poisons. *Proc. Natl. Acad. Sci. U.S.A. 102*, 6195−6200.
(37) Steen, P. W., Tian, S., Tully, S. E., Cravatt, B. F., and LeMosy, E. K. (2010) Activation of Snake in a serine protease cascade that defines the dorsoventral axis is atypical and pipe-independent in *Drosophila* embryos. *FEBS Lett. 584*, 3557−3560.
(38) Lemberg, M. K., Menendez, J., Misik, A., Garcia, M., Koth, C. M., and Freeman, M. (2005) Mechanism of intramembrane proteolysis investigated with purified rhomboid proteases. *EMBO J. 24*, 464−472.
(39) Fenyo, D., Wang, Q., DeGrasse, J. A., Padovan, J. C., Cadene, M., and Chait, B. T. (2007) MALDI sample preparation: The ultra thin layer method. *J. Visualized Exp.,* e192.
(40) Sattler, M. S., Jr., and Griesinger, C. (1999) Heteronuclear multidimensional NMR experiments for the structure determination of proteins in solution employing pulsed field gradients. *Prog. Nucl. Magn. Reson. Spectrosc. 34*, 93−158.
(41) Delaglio, F., Grzesiek, S., Vuister, G. W., Zhu, G., Pfeifer, J., and Bax, A. (1995) NMRPipe: A multidimensional spectral processing system based on UNIX pipes. *J. Biomol. NMR 6*, 277−293.
(42) Johnson, B. A. (1994) NMRView: A computer program for the visualization and analysis of NMR data. *J. Biomol. NMR 4*, 603−614.
(43) Cornilescu, G., Delaglio, F., and Bax, A. (1999) Protein backbone angle restraints from searching a database for chemical shift and sequence homology. *J. Biomol. NMR 13*, 289−302.
(44) Guntert, P. (2004) Automated NMR structure calculation with CYANA. *Methods Mol. Biol. 278*, 353−378.
(45) Linge, J. P., Williams, M. A., Spronk, C. A., Bonvin, A. M., and Nilges, M. (2003) Refinement of protein structures in explicit solvent. *Proteins 50*, 496−506.
(46) Schwieters, C. D., Kuszewski, J. J., and Clore, G. M. (2006) Using Xplor-NIH for NMR molecular structure determination. *Prog. Nucl. Magn. Reson. Spectrosc. 48*, 47−62.
(47) Schwieters, C. D., Kuszewski, J. J., Tjandra, N., and Clore, G. M. (2003) The Xplor-NIH NMR molecular structure determination package. *J. Magn. Reson. 160*, 65−73.
(48) Laskowski, R. A., MacArthur, M. W., Moss, D. S., and Thornton, J. M. (1993) PROCHECK: A program to check the steriochemical quality of protein structures. *J. Appl. Crystallogr. 26*, 283−291.
(49) Laskowski, R. A., Rullmann, J. A., MacArthur, M. W., Kaptein, R., and Thornton, J. M. (1996) AQUA and PROCHECK-NMR: Programs for checking the quality of protein structures solved by NMR. *J. Biomol. NMR 8*, 477−486.
(50) Vriend, G. (1990) WHAT IF: A molecular modeling and drug design program. *J. Mol. Graphics 8*, 29 , 52−56.
(51) Smith, P. K., Krohn, R. I., Hermanson, G. T., Mallia, A. K., Gartner, F. H., Provenzano, M. D., Fujimoto, E. K., Goeke, N. M., Olson, B. J., and Klenk, D. C. (1985) Measurement of protein using bicinchoninic acid. *Anal. Biochem. 150*, 76−85.
(52) Del Rio, A., Dutta, K., Chavez, J., Ubarretxena-Belandia, I., and Ghose, R. (2007) Solution structure and dynamics of the N-terminal cytosolic domain of rhomboid intramembrane protease from *Pseudomonas aeruginosa*: Insights into a functional role in intramembrane proteolysis. *J. Mol. Biol. 365*, 109−122.
(53) Pierrat, O. A., Strisovsky, K., Christova, Y., Large, J., Ansell, K., Bouloc, N., Smiljanic, E., and Freeman, M. (2011) Monocyclic *β*-lactams are selective, mechanism-based inhibitors of rhomboid intramembrane proteases. *ACS Chem. Biol. 6*, 325−335.
(54) Garavito, R. M., and Ferguson-Miller, S. (2001) Detergents as Tools in Membrane Biochemistry. *J. Biol. Chem. 276*, 32403−32406.
(55) Lacapere, J. J., Pebay-Peyroula, E., Neumann, J. M., and Etchebest, C. (2007) Determining membrane protein structures: Still a challenge! *Trends Biochem. Sci. 32*, 259−270.
(56) Popot, J. L. (2011) Amphipols, nanodiscs, and fluorinated surfactants: Three nonconventional approaches to studying membrane proteins in aqueous solutions. *Annu. Rev. Biochem. 79*, 737−775.
(57) Prive, G. G. (2007) Detergents for the stabilization and crystallization of membrane proteins. *Methods 41*, 388−397.
(58) Seddon, A. M., Curnow, P., and Booth, P. J. (2004) Membrane proteins, lipids and detergents: Not just a soap opera. *Biochim. Biophys. Acta 1666*, 105−117.
(59) Bondar, A. N., del Val, C., and White, S. H. (2009) Rhomboid protease dynamics and lipid interactions. *Structure 17*, 395−405.
(60) Urban, S., and Baker, R. P. (2008) In vivo analysis reveals substrate-gating mutants of a rhomboid intramembrane protease display increased activity in living cells. *Biol. Chem. 389*, 1107−1115.
(61) Wang, Y., Maegawa, S., Akiyama, Y., and Ha, Y. (2007) The role of L1 loop in the mechanism of rhomboid intramembrane protease GlpG. *J. Mol. Biol. 374*, 1104−1113.
(62) Baker, R. P., Young, K., Feng, L., Shi, Y., and Urban, S. (2007) Enzymatic analysis of a rhomboid intramembrane protease implicates transmembrane helix 5 as the lateral substrate gate. *Proc. Natl. Acad. Sci. U.S.A. 104*, 8257−8262.
(63) Urban, S., Schlieper, D., and Freeman, M. (2002) Conservation of intramembrane proteolytic activity and substrate specificity in prokaryotic and eukaryotic rhomboids. *Curr. Biol. 12*, 1507−1512.

(64) Evans, M. J., and Cravatt, B. F. (2006) Mechanism-based profiling of enzyme families. *Chem. Rev. 106*, 3279−3301.
(65) Kidd, D., Liu, Y., and Cravatt, B. F. (2001) Profiling serine hydrolase activities in complex proteomes. *Biochemistry 40*, 4005−4015.
(66) Liu, Y., Patricelli, M. P., and Cravatt, B. F. (1999) Activity-based protein profiling: The serine hydrolases. *Proc. Natl. Acad. Sci. U.S.A. 96*, 14694−14699.
(67) Blais, D. R., Lyn, R. K., Joyce, M. A., Rouleau, Y., Steenbergen, R., Barsby, N., Zhu, L. F., Pegoraro, A. F., Stolow, A., Tyrrell, D. L., and Pezacki, J. P. (2010) Activity-based protein profiling identifies a host enzyme, carboxylesterase 1, which is differentially active during hepatitis C virus replication. *J. Biol. Chem. 285*, 25602−25612.
(68) Urban, S., and Wolfe, M. S. (2005) Reconstitution of intramembrane proteolysis in vitro reveals that pure rhomboid is sufficient for catalysis and specificity. *Proc. Natl. Acad. Sci. U.S.A. 102*, 1883−1888.
(69) Baker, R. P., and Urban, S. (2012) Architectural and thermodynamic principles underlying intramembrane protease function. *Nat. Chem. Biol. 8*, 759−768.
(70) Ye, Y., and Godzik, A. (2003) Flexible structure alignment by chaining aligned fragment pairs allowing twists. *Bioinformatics 19* (Suppl. 2), 246−255.
(71) Prlic, A., Bliven, S., Rose, P. W., Bluhm, W. F., Bizon, C., Godzik, A., and Bourne, P. E. (2010) Pre-calculated protein structure alignments at the RCSB PDB website. *Bioinformatics 26*, 2983−2985.
(72) Finn, R. D., Tate, J., Mistry, J., Coggill, P. C., Sammut, S. J., Hotz, H. R., Ceric, G., Forslund, K., Eddy, S. R., Sonnhammer, E. L., and Bateman, A. (2008) The Pfam protein families database. *Nucleic Acids Res. 36*, D281−D288.
(73) Yang, J. C., Van Den Ent, F., Neuhaus, D., Brevier, J., and Lowe, J. (2004) Solution structure and domain architecture of the divisome protein FtsN. *Mol. Microbiol. 52*, 651−660.
(74) Arends, S. J., Williams, K., Scott, R. J., Rolong, S., Popham, D. L., and Weiss, D. S. (2010) Discovery and characterization of three new *Escherichia coli* septal ring proteins that contain a SPOR domain: DamX, DedD, and RlpA. *J. Bacteriol. 192*, 242−255.
(75) Gerding, M. A., Liu, B., Bendezu, F. O., Hale, C. A., Bernhardt, T. G., and de Boer, P. A. (2009) Self-enhanced accumulation of FtsN at Division Sites and Roles for Other Proteins with a SPOR domain (DamX, DedD, and RlpA) in *Escherichia coli* cell constriction. *J. Bacteriol. 191*, 7383−7401.
(76) Ursinus, A., van den Ent, F., Brechtel, S., de Pedro, M., Holtje, J. V., Lowe, J., and Vollmer, W. (2004) Murein (peptidoglycan) binding property of the essential cell division protein FtsN from *Escherichia coli*. *J. Bacteriol. 186*, 6728−6737.
(77) Clemmer, K. M., Sturgill, G. M., Veenstra, A., and Rather, P. N. (2006) Functional characterization of *Escherichia coli* GlpG and additional rhomboid proteins using an *aarA* mutant of *Providencia stuartii*. *J. Bacteriol. 188*, 3415−3419.
(78) Chung, H. S., Yao, Z., Goehring, N. W., Kishony, R., Beckwith, J., and Kahne, D. (2009) Rapid β-lactam-induced lysis requires successful assembly of the cell division machinery. *Proc. Natl. Acad. Sci. U.S.A. 106*, 21872−21877.
(79) Richardson, J. S., and Richardson, D. C. (1988) Amino acid preferences for specific locations at the ends of α helices. *Science 240*, 1648−1652.
(80) Cole, C., Barber, J. D., and Barton, G. J. (2008) The Jpred 3 secondary structure prediction server. *Nucleic Acids Res. 36*, W197−W201.
(81) Jeyaraju, D. V., McBride, H. M., Hill, R. B., and Pellegrini, L. (2011) Structural and mechanistic basis of Parl activity and regulation. *Cell Death Differ. 18*, 1531−1539.
(82) Hill, R. B., and Pellegrini, L. (2010) The PARL family of mitochondrial rhomboid proteases. *Semin. Cell Dev. Biol. 21*, 582−592.
(83) Carruthers, V. B., and Blackman, M. J. (2005) A new release on life: Emerging concepts in proteolysis and parasite invasion. *Mol. Microbiol. 55*, 1617−1630.
(84) Urban, S. (2009) Making the cut: Central roles of intramembrane proteolysis in pathogenic microorganisms. *Nat. Rev. Microbiol. 7*, 411−423.